Supplementary Information

Table S1. Reports on both peroxo-vanadium structures determined by X-ray crystallographic analysis and catalytic reactivity in the same articles.

entry	reactive peroxo-vanadium species	catalytic reaction	ref.
1	$\{^{n}Bu_4N\}_3[V_{12}O_{30}(OO^{t}Bu)F_2]$	epoxidation of alkenes bromination of alkenes and chlorodimedone	This work
2	$VO(O_2)(PAH)(phen)$	bromination of olefinic alcohols	S1
3	$\{^{n}Bu_4N\}[VO_2(pca)_2]$	oxidation of alkane	S2
4	$[VO(O_2)(Byim)(MeOH)]ClO_4$	bromination of aromatic alcohols	S3
5	$\{^{n}Bu_4N\}[\{Ph_3SiO\}_2VO(O_2)]$	oxidation of 2-methylcyclohexanone	S4
6	$\{NH_4\}[VO(O_2)(mpa)]$ $K_2[VO(O_2)nta]$ $K[VO(O_2)Hheida]$	bromination of aromatic substrate	S5
7	$K[VO(O_2)ada]$ $[VO(O_2)bpg$ $[VO(O_2)tpa]ClO_4]$	halide oxidation	S6
8	$KVO(O_2)Hheida$	halogenation of Phenol Red	S7

PAHH = *N*-(1-phenyl acetyl acetyl)hydroxamic acid, phen = phenanthroline, Hpca = pyrazine-2-carboxylic acid, Byim = 2,6-di(1*H*-benzo[d]imidazole-2-yl)pyridine, dipic = pyridinedicarboxylate, mpa = 4-methoxypicolinamide, H_3nta = nitrilotriacetic acid, H_3neida = *N*-(2-hydroxyethyl)iminodiacetic acid, H_2ada = *N*-(2-amidomethyl)iminodiacetic acid, Hbpg = *N*,*N*-bis(2-pyridylmethyl)glycine, tpa = *N*, *N*, *N*-tris(2-pyridylmethyl)amine,

Table S2. Reported fluoride-incorporated polyoxovanadates.

entry	anion formula	coorditnation geometry of vanadium atoms	ref.
1	$[V_{12}O_{30}(O^tBu)F_2]^{3-}$	Square pyramid, Tetrahedron	This work
2	$[V_{12}O_{30}(acac)F_2]^{3-}$	Square pyramid	This work
3	$[V_{12}O_{30}(OO^tBu)F_2]^{3-}$	Square pyramid	This work
4	$[V_7O_{19}F\{(CH_2)_3CCH_2OH\}^{4-}$	Square pyramid, Tetrahedron	46
5	$[V_{12}O_{30}F_2\{(CH_2)_3CCH_2OH\}_2]^{6-}$	Square pyramid	46
6	$[V_{10}O_{28}F_2\{(CH_2)_3CCH_2OH\}_2]^{4-}$	Square pyramid	46
7	$[V_7O_{19}F]^{4-}$	Square pyramid, Tetrahedron	44
8	$[HV_{11}O_{29}F_2]^{4-}$	Square pyramid	35
9	$[V_{10}O_{30}F_2]^{4-}$	Square pyramid	43,S8
10	$[V_{12}O_{30}F_4(H_2O)_2]^{4-}$	Square pyramid	47
11	$[V_{14}O_{36}F_4]^{8-}$	Square pyramid, tetrahedron, trigonal bipuramid	48
12	$[V_{14}O_{36}F_2(L)_2]^{6-}$	Square pyramid, tetrahedron, trigonal bipuramid	49
13	$[V_{14}O_{34}F_6]^{4-}$	Square pyramid, tetrahedron, trigonal bipyramid	50
14	$[V_2O_{30}F_2(pic)_2]^{6-}$	Square pyramid	50
15	$[Bi_2(DMSO)_6V_{10}O_{28}F_2]^{3-}$	Square puramid	41
16	$[\{Pd(NO_3)(DMSO)\}_2V_{12}O_{32}(F)_2]^{4-}$	Square pyramid, tetrahedron	43
	different structures from above polyoxovanadates		
17	$[V_4O_8(glut)_2F]^-$		S9
18	$[V_6O_6F(OH)_3\{(OCH_2)_3CCH_3\}_3]^-$		51
19	$[V_{16}O_{38}F]^{4-}$	Square pyramid	32

L = pyridine, pyrazine, imidazole. pic = picolinate. DMSO = dimethyl sulfoxide. glut = glutarate

Table S3. Crystallographic data for V12-O^{t}Bu, V12-acac and V12-OO^{t}Bu

	V12-O^{t}Bu	V12-acac	V12-OO^{t}Bu
formula	$C_{113}H_{252}F_4N_6O_{71}V_{24}$	$C_{59}H_{126}F_2N_4O_{34}V_{12}$	$C_{104}H_{234}F_4N_6O_{64}V_{24}$
fw	4129.75	2084.91	3891.52
crystal system	monoclinic	monoclinic	orthorhombic
space group	$P2_1/n$ (#14)	$P2_1/n$ (#14)	$Pca2_1$ (#29)
a (Å)	15.7550(3)	17.7995(4)	17.1990(4)
b (Å)	25.4335(4)	23.6442(5)	21.6914(5)
c (Å)	21.5604(4)	20.9424(4)	54.0590(12)
β (deg)	92.2530(10)	91.9450(10)	90
V (Å^3)	8632.7(3)	8808.6(3)	20167.8(8)
Z	2	4	8
μ (mm^{-1})	11.096	10.872	9.441
R_1 ($I > 2\sigma(I)$)	0.0358	0.0559	0.0905
wR_2	0.0925	0.1455	0.2254

Table S4. Comparison of the catalytic performance for the epoxidation of cyclooctene with ^{t}BuOOH as an oxidant with previously reported polyoxometalate catalysts.

entry	catalyst	molar ratio cat:substrate:oxidant	temp. / ºC	time / h	selectivity of epoxide	TON	ref.
	polyoxometalate catalyst						
1	$[V_{12}O_{30}(O^{t}Bu)F_2]^{3-}$	0.0083:1:1	32	2.5	>99%	105	This work
2	$Cs_7[PW_{10}Cu_2(H_2O)_2O_{38}]\cdot 9H_2O$	unknown (15mg):1:1.5	60	20	81%	851	S10
3	$\{Hptz\}_4[SiMo_{12}O_{40}]$	0.01:1:1.5	70	24	>99%	100	S11
4	$\{(n\text{-hexyl})_4N\}_4[Mo_2O_2((2\text{-OPh})CH{=}NCH_2CH_2CH_2Si)_2\text{-}SiW_{11}O_{39}]$	0.02:1:3	75	6	>99%	50	S12
5	$\{(n\text{-hexyl})_4N\}_4[Mo_2O_2(acac)(NH_2CH_2CH_2CH_2Si)_2\text{-}SiW_{11}O_{39}]$	0.0016:1:3	75	8	>99%	62	S13
6	15 wt% Vanadomolybdophosphoric acids wet-impregnated on hydrated titania	0.01:2	80	5	>99%	1150	S14
7	$CP_3[PMo_{12}O_{40}]$	0.000002:1:1.5	80	24	53.1%	12000	S15
8	$C_{15}H_{34}MoN_6O_{43}SiW_{11}$	0.0042:1:2.24	reflux	0.5	>99%	170	S16
9	$[H(C_{10}H_{10}N_2)Cu_2][PMo_{12}O_{40}]$	0.0002:1:0.4	85	12	80%	3000	S17
10	$H_4[SiMo_{12}O_{40}]$ employed to support on amine functionalized Hydrous zirconia nanoparticles	0.0093:1:2	reflux	2	98% yield	105	S18
11	$H_3[PMo_{12}O_{40}]$ employed to support on on amine functionalized Boehmite nanoparticles	0.0157:1:2	reflux	0.25	98% yield	62	S19
12	$\{Bu_4N\}_2[Mo_6O_{19}]$	0.00025:1:2	80	6	87%	123	S20
13	$[Ni_2(fsa)_7(H_2O)(SiMo_{12}O_{40})]$	0.0006:1:0.017	80	48	97.21%	117	S21
14	$[Mo_{36}(NO)_4O_{108}(H_2O)_{16}]^{12-}$ on amine functionalized SBA-15	0.0045:1:2	reflux	1.5	98%	220	S22
15	$[H(atrz)]_4[(atrz)_2(Mo_8O_{26})]$	0.005:1:1	45	12	>99%	184	S23
16	$(NH_4)_{12}[Mo_{36}(NO)_4O_{108}(H_2O)_{16}]$ supported on the clinoptilolite zeolite	0.0005:1:2	reflux	3	>99%	1800	S24
17	$[PMo_{10}V_2O_{40}]^{5-}$ immobilized on ionic liquid-modified MCM-41	0.006:1:0.01	reflux	25	90%	276	S25

ptz = 5-(2-pyridyl)tetrazole, CP = 1-butylpyridinium, fsa = bis(4chlorophenyl)propyl triazolee, atrz = 3-amino-1,2,4-triazole

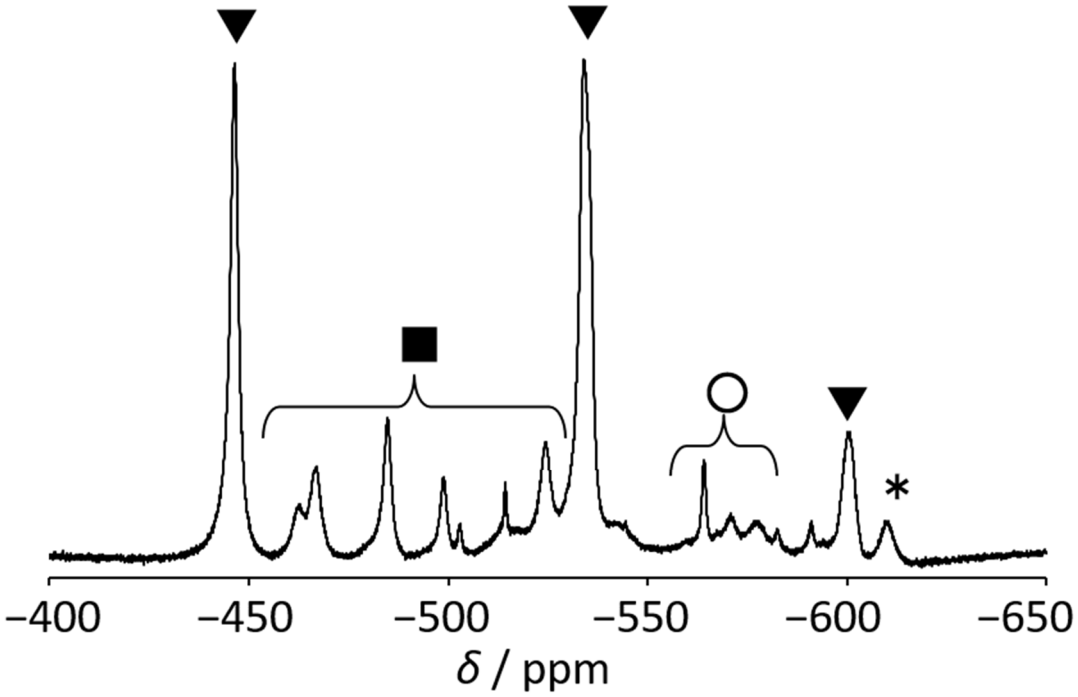

Figure S1. ^{51}V NMR spectrum after the reaction of $\{^{n}Bu_4N\}_4[V_{12}O_{32}(CH_3NO_2)]$ with 1.5 equiv. of $\{^{n}Bu_4N\}F$ in nitromethane. The triangles, square, circle and asterisk represent the peaks due to V7, V11, $[V_{12}O_{32}(CH_2NO_2)]^{5-}$ and $[V_5O_{14}]^{4-}$, respectively. The reaction conditions were same as those of the previously reported anion insertion into dodecavanadates[S26] $[V_{12}O_{32}(CH_2NO_2)]^{5-}$ was formed because of proton removal by the effect from the basicity of $\{^{n}Bu_4N\}F$.[S27]

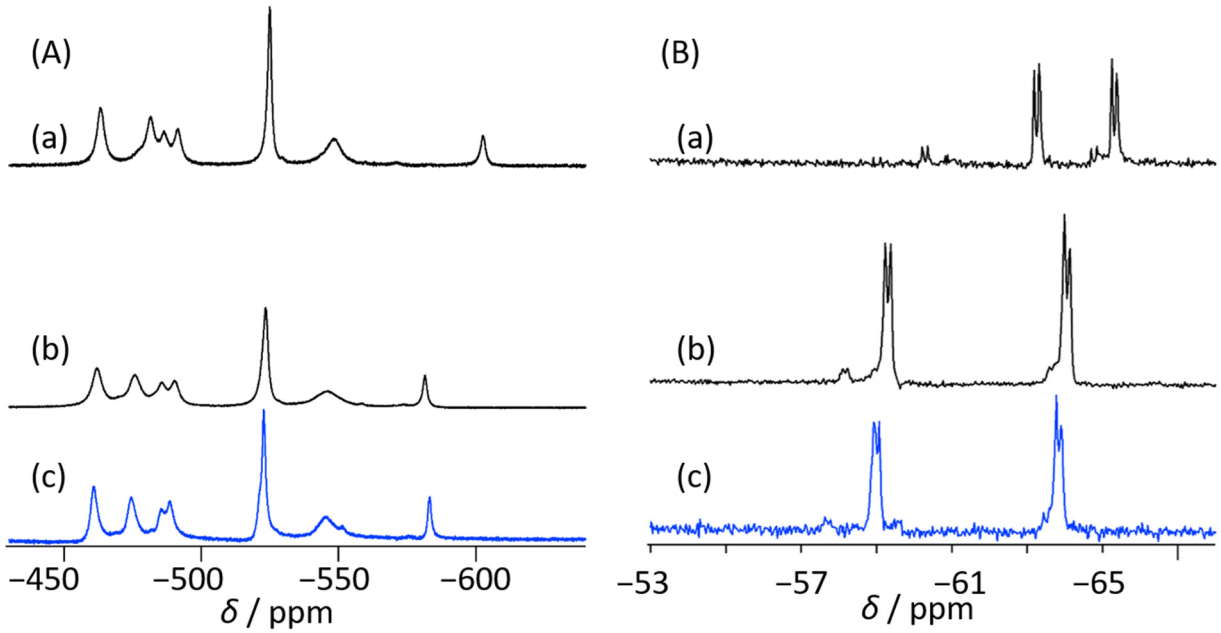

Figure S2. (A) ^{51}V and (B) ^{19}F NMR spectra of V12-OO^{t}Bu (a) before and (b) after the quantitative reaction with cyclooctene. Spectra (c) are those of the authentic sample of V12-O^{t}Bu. Reaction conditions: cyclooctene 1 mmol, CD_3NO_2 2 mL, V12-OO^{t}Bu 0.077 mmol, naphthalene 0.2 mmol, 90 min, 25ºC. 90% yield of cyclooctene oxide based on V12-OO^{t}Bu was detected in GC.

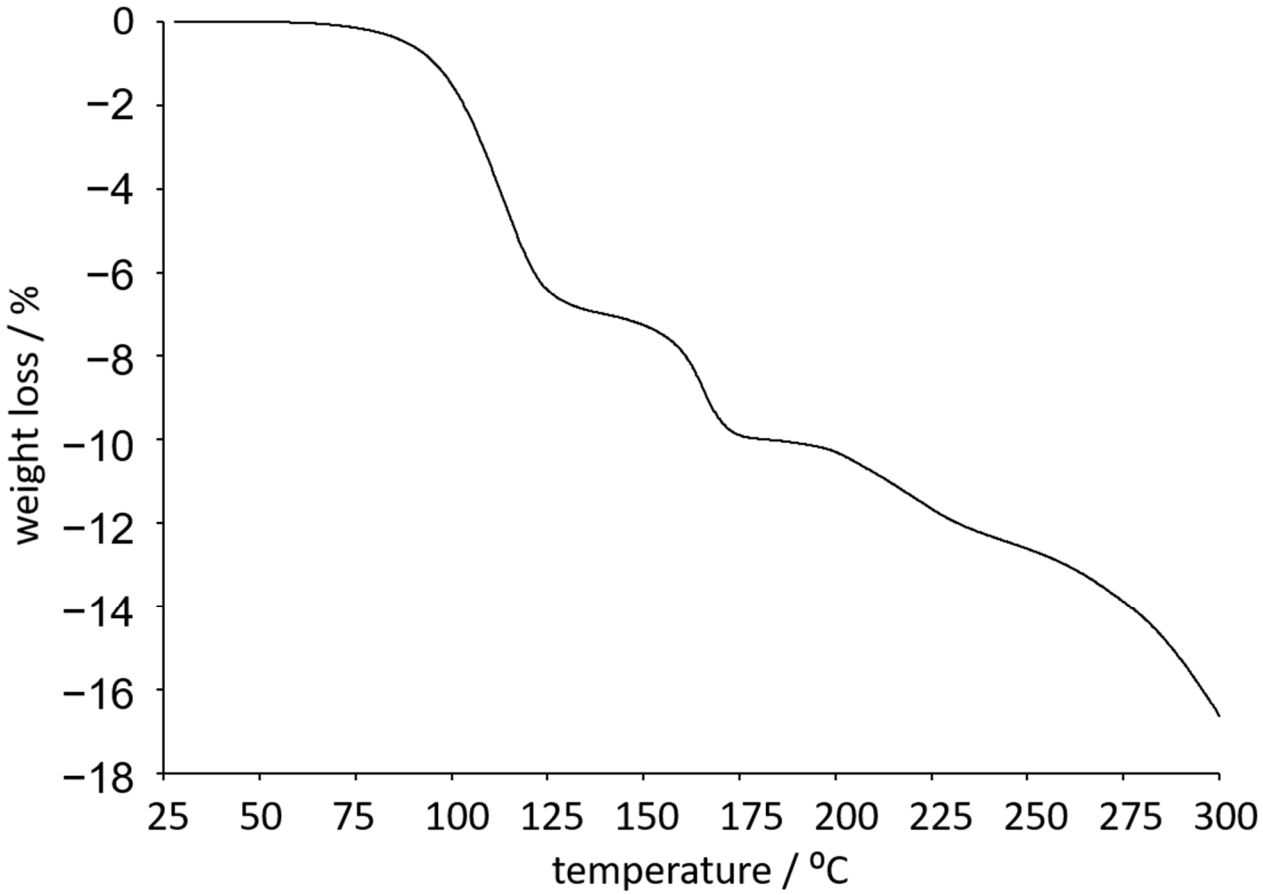

Figure S3. TG data of V12-O^{t}Bu. The first step of the weight loss is −6.58% at 127 ºC due to 1.5 molecules of $(CH_3)_2CO_3$ and the second one is −10.06 % at 187 ºC due to 1 molecule of ^{t}BuOH. The weight loss over 200 ºC is due to the decomposition of tetra-*n*-butylammonium.

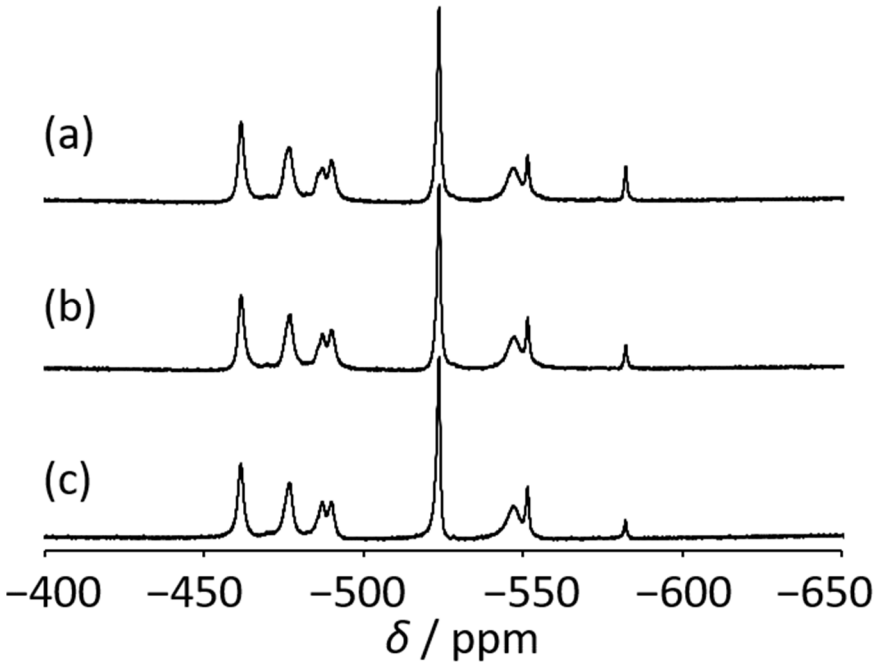

Figure S4. ^{51}V NMR spectra of V12-O^{t}Bu in the presence of (a) 1, (b) 1.5 and (c) 2 equiv. of ^{i}PrOH in acetonitrile.

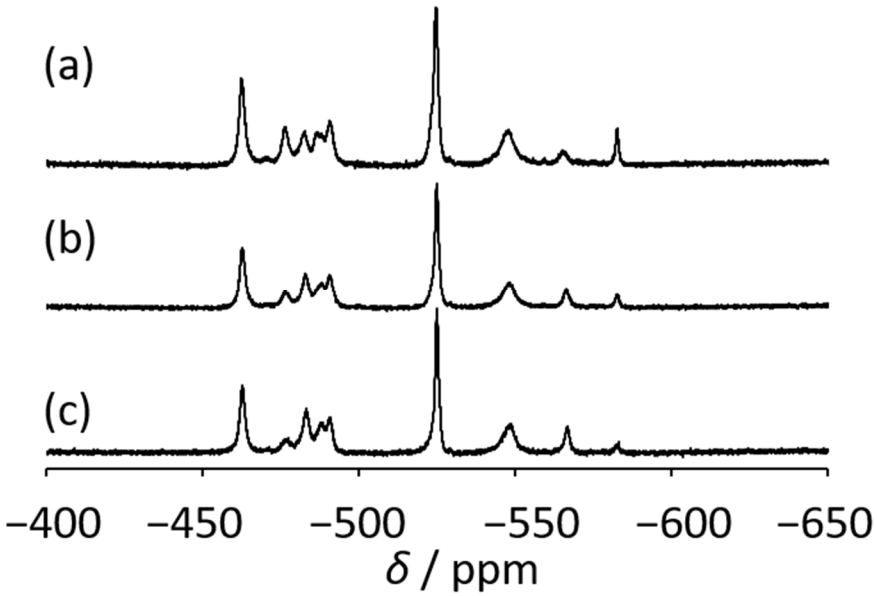

Figure S5. ^{51}V NMR spectra of V12-O^{t}Bu in the presence of (a) 2, (b) 5 and (c) 10 equiv. of AcOH in acetonitrile.

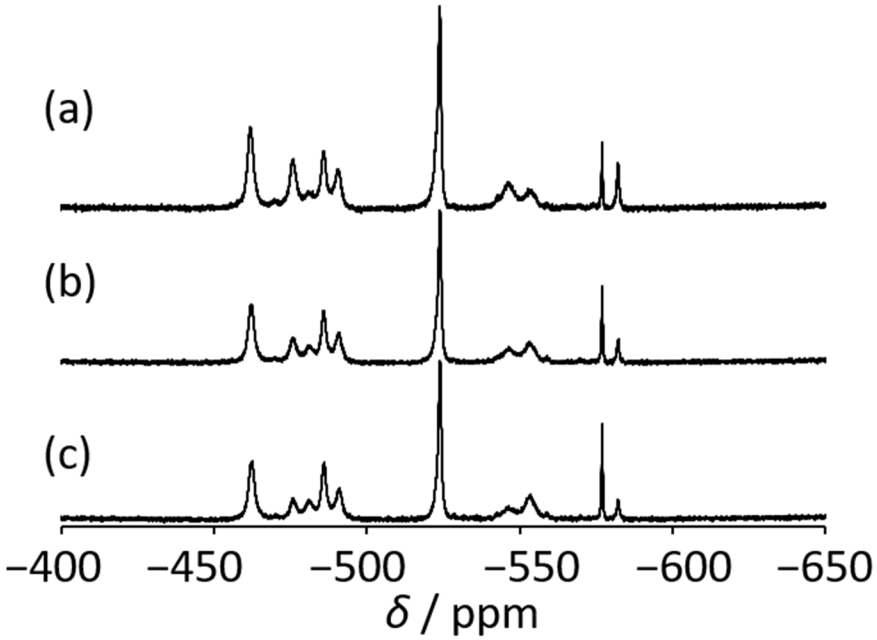

Figure S6. ^{51}V NMR spectra of V12-O^{t}Bu in the presence of (a) 0.4, (b) 0.6 and (c) 0.8 equiv. of acacH in acetonitrile.

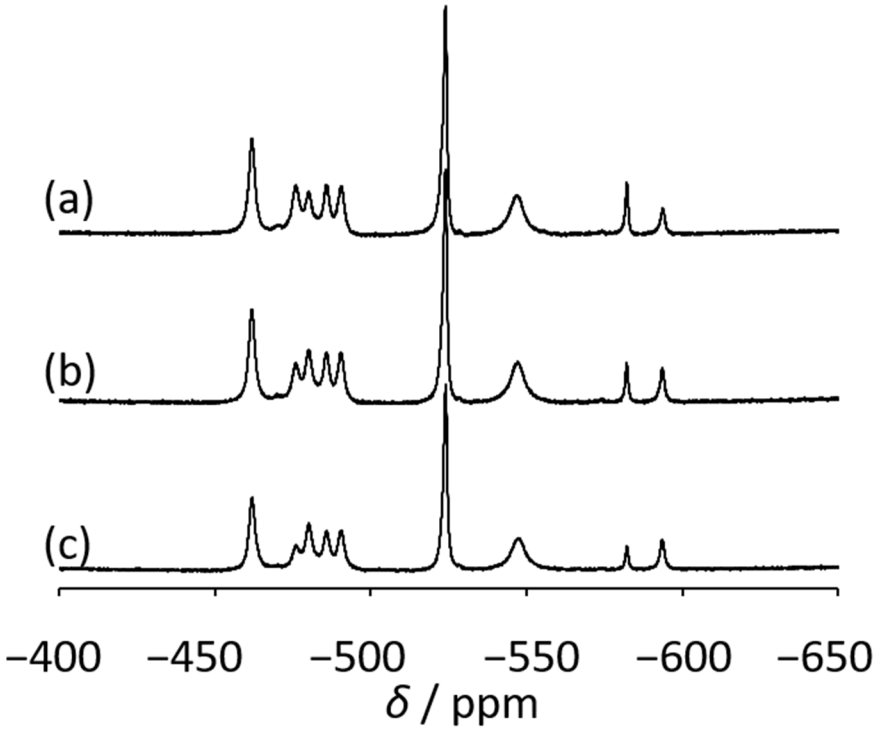

Figure S7. ^{51}V NMR spectra of V12-O^{t}Bu in the presence of (a) 2.8, (b) 5.5 and (c) 11 equiv. of ^{t}BuOOH in acetonitrile. The lowest peak of V12-OO^{t}Bu was shifted probably due to the different solvent system.

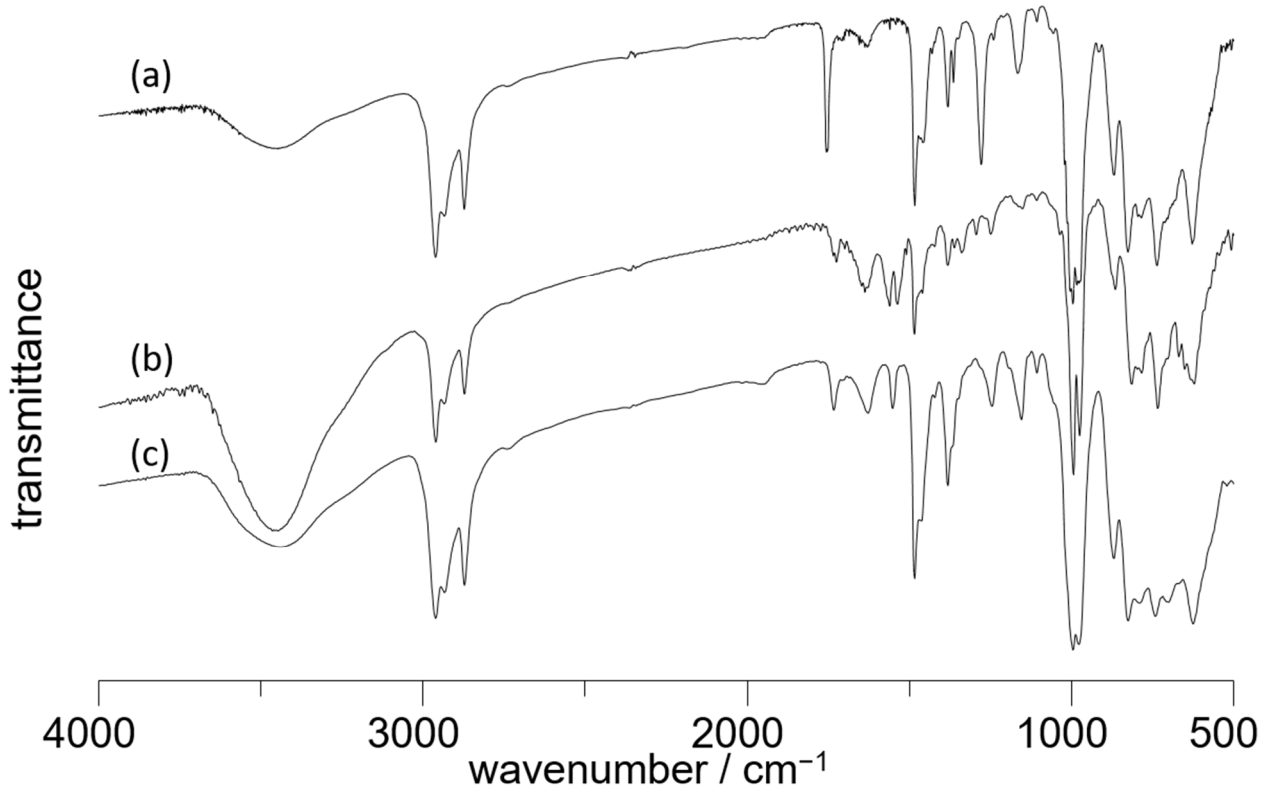

Figure S8. IR spectra of (a) V12-O^{t}Bu, (b) V12-acac and (c) V12-OO^{t}Bu.

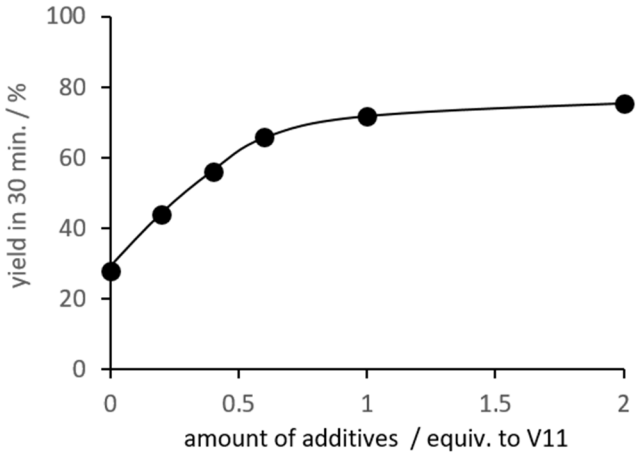

Figure S9. Yield in 30 min for epoxidation of cyclooctene as a function of the amount of added TsOH. Reaction conditions: Cyclooctene (1 mmol), ^{t}BuOOH (5.5 M in decane, 1 mmol), V11 (9.1 μmol), propylene carbonate/dichloromethane 2 mL (1:1. v/v), TsOH (0−2 equiv. to V11), naphthalene (0.2 mmol, internal standard), 32°C. Yields were determined by GC. With an increase in the amount of added p-toluenesulfonic acid (TsOH) with respect to V11, the yield of cyclooctene oxide in 0.5 h gradually increased and reached a plateau after further addition of more than 1 equiv. of TsOH.

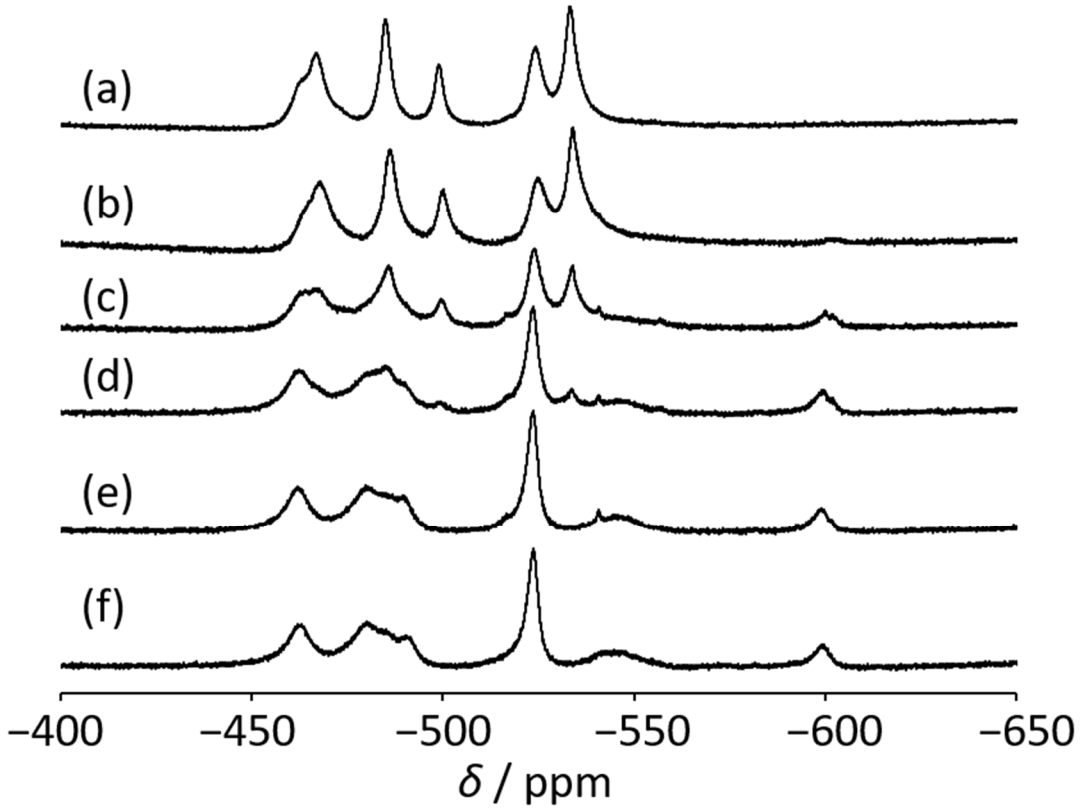

Figure S10. ^{51}V NMR spectra of V11 (a) without and with 100 equiv. of ^{t}BuOOH in the presence of (b) 0, (c) 0.4, (d) 0.8, (e) 1.3 and (f) 1.8 equiv. of TsOH with respect to V11. Without addition of acid, signals due to alkyoperoxo-vanadium species were not observed.

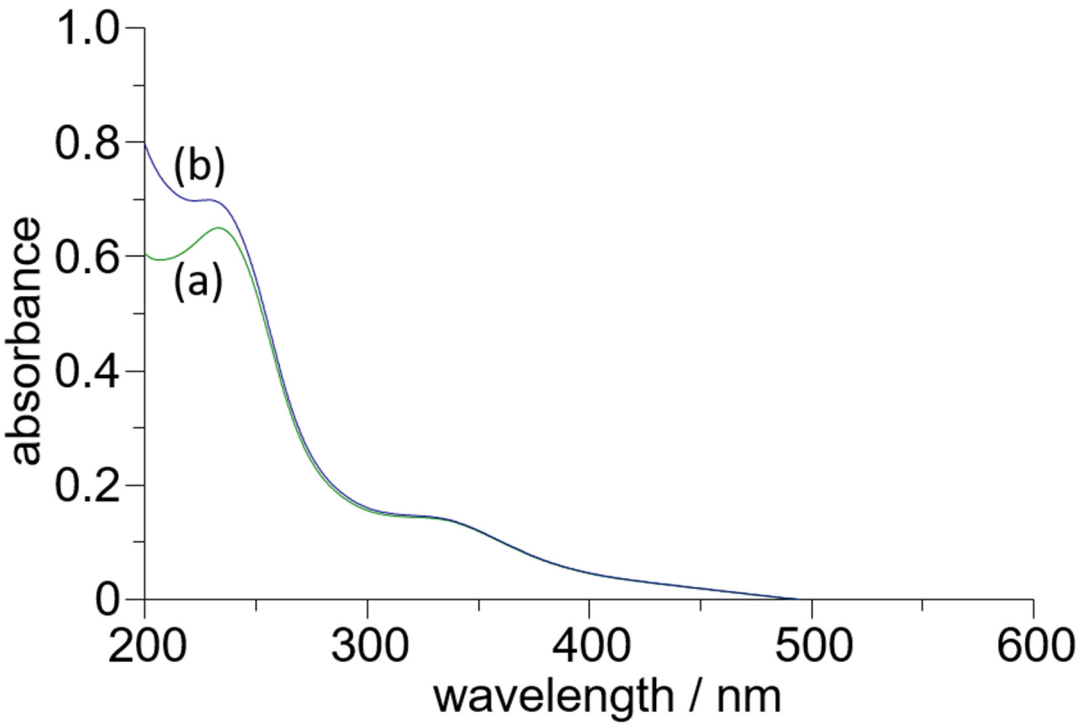

Figure S11. UV-vis spectra of acetonitrile solution of V12-O^{t}Bu (a) before and (b) after addition of 100 equiv. of 5.5 M ^{t}BuOOH in decane solution. The concentration of V12-O^{t}Bu was 1.5 x 10^{-5} M.

Additional references

S1. T. K. Si, S. S. Paul, M. G. B. Drew, K. K. Mukherjea, *Dalton Trans*. 2012, **41**, 5805-5815.

S2. G. Süss-Fink, S. Stanislas, G. B. Shulpin, G. V. Nizova, H. Stockli-Evans, A. Neels, C. Bobillier, S. Claude, *J. Chem. Soc. Dalton Trans*. 1999, 3169-3175.

S3. E. Palmajumder, S. Patra, M. G. B. Drew, K. K. Mukherjea, *New J. Chem*. 2016, **40**, 8696-8703.

S4. M. Vennat, J.-M. Brégeault, P. Herson, *Dalton Trans*. 2004**,** 908-913.

S5. P. Chen, S. Zhang, J. Zhang, W. Xia, X. Yu, *J. Coord. Chem*. 2019, **72**, 239-250.

S6. G. J. Colpas, B. J. Hamstra, J. W. Kampf, V. L. Pecorao, *J. Am. Chem. Soc*. 1996, **118**, 3469-3478.

S7. G. J. Colpas, B. J. Hamstra, J. W. Kampf, V. L. Pecoraro, *J. Am. Chem. Soc.* 1994, **116**, 3627-3628.

S8. A. Müller, R. Rohlfing, A.-L. Barra, D. Getteschi, *Adv. Mater*. 1993, ***5***, 915-919.

S9. M. Gómez, A. Pastor, E. Álvarez, J. L. Olloqui-Sariego, A. Gailindo, *Dalton Trans*. 2018, **47**, 2183-2191.

S10. A. Patel, R. Sadasivan, *Inorg. Chim. Acta* 2017, **485**, 101-108.

S11. M. S, Nunes, P. Neves, A. C. Gomes, L. Cunha-Silva, A. D. Lopes, A. A. Valente, M. Pillinger, I. S. Gonçalves, *Inorg. Chim. Acta* 2021, **516**, 120129.

S12. M. Moghadam, V. Mirkhani, S. Tangestaninejad, I. Mohammadpoor-Baltork, M. M. Javadi, *Polyhedron*, 2010, **29**, 648-654.

S13. M. Moghadam, V. Mirkhani, S. Tangestaninejad, I. Mohammadpoor-Baltork, M. M. Javadi, *Inorg. Chim. Acta* 2010, **13**, 244-249.

S14. R. H. Ingle, A. Vinu, S. B. Halligudi, *Catal. Commun*. 2008, **9**, 931-938.

S15. B. Guérin, D. M. Fernandes, J.-C. Daran, D. Agustin, R. Poli, *New J. Chem.* 2013, **37**, 3466-3475.

S16. S. S. Hosseinyzade, F. M. Zonoz, B. Bahramian, *Catal. Lett*. 2018, **148**, 1324-1335.

S17. S. Roy, V. Vemuri, S. Maiti, K. S. Manoj, U. Subbarao, S. C. Peter, *Inorg. Chem.* 2018, **57**, 12078-12092.

S18. M. Mirzaee, B. Bahramian, M. Shahraki, H. Moghadam, A. Mirzaee, *Catal. Lett*. 2018, **148**, 3003-3017.

S19. M. Mirzaee, B. Bahramian, A. Ashrafian, A. Amoli, *Appl. Organomet. Chem.* 2018, **32**, e4011.

S20. J. Pisk, B. Prugovečki, D. Matkvić-Čalogović, T. Jednačak, P. Novak, D. Agustin, V. Vrdoljak, *RSC adv*. 2014, **4**, 39000-39010.

S21. L. Zhou, J. Liu, W. Ji, H. Huang, H. Hu, Y. Liu, Z. Kang, *J. Mater. Chem. A* 2014, **2**, 12686-12691.

S22. M. Bagherzadeh, H. Hosseini, S. Akbayrak, S. Özkar, *ChemistrySelec*. 2019, **4**, 5911-5917.

S23. H. Gao, J. Yu, J. Du, H. Niu, J. Wang, X. Song, W. Zhang, M. Jia, *J. Clust. Sci*. 2014, **25**, 1263-1272.

S24. M. Bagherzadeh, H. Hosseini, *J. Coord. Chem.* 2017, **70**, 2212-2223.

S25. R. Hajian, S. Tangestaninejad, M. Moghadam, V. Mirkhani, I. Mohammadpoor-Baltork, A. R. Khosropour, *J. Coord. Chem.* 2011, **64**, 4134-4344.

S26. S. Kuwajima, Y. Kikukawa, Y. Hayashi, *Chem. Asian J*. 2017, **12**, 1909-1914.

S27. Y. Kikukawa, H. Kitajima, S. Kuwajima, Y. Hayashi, *Molecules* 2020, **25**, 5670.